FROM CARBON DIOXIDE TO METHANE VIA CRYSTALLIZED HYDROGEN CARBONATE

Friedrich Waag[1]*, Christoph Wieland[1,2]

[1]University of Duisburg-Essen, Chair of Energy Process Engineering and Energy Systems, Essen, Germany

[2]Gas- und Wärme-Institut Essen e.V., Essen, Germany

*Corresponding Author: friedrich.waag@uni-due.de

ABSTRACT

Can mankind reduce carbon dioxide emissions fast enough by switching to renewable energies to stop significant global warming with all its consequences? The answer is either an optimistic "maybe" or a realistic "no". A plan B is needed. Further solutions to actively reduce carbon dioxide emissions are needed. Chemical absorption processes for carbon dioxide based on aqueous amine solutions are already well developed due to their historical importance in gas purification and can be used downstream of strong carbon dioxide emitters. However, there are still economic hurdles for a broad retrofitting of such systems, which are due to rapidly degrading and energy-intensive absorber solutions during desorption. This work addresses these problems by using a potassium carbonate solution with various promoters. In addition, an alternative, thermal desorption process is presented, which is preceded by the crystallization and drying of the easily storable and transportable potassium hydrogen carbonate. This creates new spatial and temporal flexibility in the use of the process. To demonstrate the use of carbon dioxide, its release through thermal decomposition of the hydrogen carbonate and its subsequent hydrogenation to methane are being investigated.

1 INTRODUCTION

Mankind emitted the new record of 36.1 Gt of carbon dioxide (CO_2) to Earth's atmosphere in 2022 with the sectors power and industry accounting for about 40% and 30%, respectively (Liu *et al.*, 2023). The average annual growth in emissions over the last 30 years was 1.8% and has to meet -4% per year for the next 30 years to reach the goal of 2 K average global warming (Liu *et al.*, 2022). The transition of primary energy supply to renewable sources may take longer than this and the effects of climate change are already being felt. Quickly implementable solutions are needed to reduce CO_2 emissions. Post-combustion or, more generally, post-CO_2-emission approaches interfere the least with existing (power) technology and are therefore the fastest to implement, simply by retrofitting. Furthermore, chemical absorption of CO_2 in liquid media is considered to be the most promising technology due to its flexibility with regard to the parameters of the gas supply, in particular the volume flow and the CO_2 concentration (Ochedi *et al.*, 2021).

Until the 1930s, scientists investigated the solubility of CO_2 in aqueous solutions particularly out of curiosity and to understand natural processes like photosynthesis or the interaction of the atmosphere and oceans. Studies focused on alkaline carbonate solutions as absorbents (McCoy and Smith, 1911; Williamson and Mathews, 1924). The increasing demand for CO_2 in the chemical industry led to greater research interest in the coming decades, particularly in the desorption of pure CO_2 from absorber solutions. In addition to carbonates, ammonia and hydroxides, amines with faster absorption rates and higher loading capacities attracted particular attention as absorbents (Hirst and Pinkel, 1936; Astarita *et al.*, 1964; Hikita *et al.*, 1979).

https://doi.org/10.52202/077185-0132

Research interest continuously grows from the 1980s with the knowledge about the influence of humans on global warming caused by high CO_2 emissions. Amines have established themselves as absorbents and are usually used in aqueous solutions at some 10 wt.-%. Compromises between CO_2 loading capacity, which is higher for multinary amines, and reactivity, which in turn is higher for primary amines, can be addressed with blends of different amines (Aghel *et al.*, 2022). In addition, further increase in reactivity can be achieved with increasing steric hindrance, as less-stable carbamates are formed during CO_2 absorption (Sartori and Savage, 1983; Hook, 1997). However, amines are generally subject to thermal and oxidative degradation, which leads to the loss of detergent and causes corrosion of plant components due to degradation products (Gouedard *et al.*, 2012). Amino acids have the same functional groups as amines, but are significantly more resistant. They are therefore increasingly being investigated as an alternative to amines (Sang Sefidi and Luis, 2019).

Aqueous solutions of mineral carbonates, especially potassium carbonate (K_2CO_3) at some 10 wt.-%, continue to be investigated as absorbents despite their poorer performance compared to amines or amino acids, certainly for economic and ecologic reasons. However, early studies have also shown that small amounts of an amine significantly improve the absorption properties of carbonates (Killeffer, 1937; Tseng *et al.*, 1988). For example, when using a K_2CO_3 solution with piperazine as promoter, the CO_2 capacity can be exceeded by 50% compared to monoethanolamine under comparable conditions and at a relevant scale, while saving 25% to 46% of the energy (Culliane *et al.*, 2005). The enhancing effect can also be achieved with various amino acids or their salts (Ahmed and Wiheeb, 2020).

In this study, the approach of the K_2CO_3 absorption medium promoted with amines or amino acids was studied as well as the influence of additional reagents such as hydroxides and glycols. Furthermore, the desorption of CO_2 from the absorption medium was replaced with a multi-stage process in which the potassium hydrogen carbonate ($KHCO_3$) formed was crystalized, dried and then thermally decomposed to get CO_2 as main product, K_2CO_3 for absorber refreshing and water as byproduct. Crystallization and drying yields a robust CO_2 storage with high volume density, which can be easily transported and also be used in applications other than the supply of pure CO_2. Thanks to the good storage and transport properties of the dry $KHCO_3$, processes can be separated very well in terms of space and time in a typical adsorption-desorption application. The additional flexibility makes the use of post-combustion or post-CO_2-generation technologies for CO_2 emission reduction even more attractive. To close the circle, the use of CO_2 as feedstock in its hydrogenation to methane (CH_4) over a commercial ruthenium-aluminum oxide catalyst was demonstrated.

2 MATERIALS AND METHODS

Experimental studies using laboratory-scale test setups were conducted as described here along the steps of the process chain. Figure 1 schematically shows the different setups and puts them in the context of the overall process.

2.1 Chemical Absorption of CO_2 in Aqueous K_2CO_3 Solutions

A temperature-controlled, wetted-wall column reactor was used to study the interaction of CO_2 and different liquid absorption media at the gas-liquid interface. Characteristic dimensions of the reactor were 30 mm inner diameter and 114 mm height of the outer column and 20 mm inner diameter and 96 mm height of the inner column. The gas flows into the outer column from below through four circular openings with a diameter of 3 mm. The absorption medium, which previously flowed laminar down the outer wall of the inner column, leaves the outer column through the same number of similar openings. In all absorption experiments, a gas mixture of 14 vol% CO_2 in nitrogen (N_2) was used, which flowed through the reactor at 20 l/h, controlled by calibrated mass flow controllers (EL-FLOW Select, Bronkhorst High-Tech BV, Ruurlo, The Netherlands). Downstream of the reactor, the gas was dried in a cooler (CGEK 5, Hartmann & Braun AG, now ABB Ltd, Zurich, Switzerland) and analyzed with measuring devices (INFRA.sens, Wi.Tec - Sensorik GmbH, Wesel, Germany or Carbondio-030, Angst+Pfister Sensors and Power AG, Zurich, Switzerland) based on non-diffractive infrared sensors. The measuring devices were zeroed with pure N2 and calibrated with the aforementioned CO_2 gas

https://doi.org/10.52202/077185-0132

mixture. The absorption medium was circulated at 60 l/h between the reactor and the storage vessel using a gear pump. The supplied absorption medium and the reactor were tempered to 293 K, unless otherwise specified.

The mass transfer rate r was calculated with Equation (1) from the molar flow density J and the partial pressure of CO_2 p. The molar flow density is mainly determined by the applied volume flow rate, absorbed CO_2 and the reactor geometry. The partial pressure in this case is the average logarithmic partial pressure in order to take into account the change in partial pressure due to absorption and the logarithmic trend of the decrease.

$$r = J / p \tag{1}$$

All absorption media investigated were based on desalinated water and K_2CO_3 (≥99, Ph. Eur., Carl Roth Gmbh + Co. KG, Karlsruhe, Germany). Various additives were used in different amounts to manipulate the mass transfer rate of CO_2. The promoters were the amine piperazine (PZ; ReagentPlus, 99%, Sigma Aldrich, St. Louis, United States), the alkanolamine 2-amino-2-methyl-1-propanol (AMP; ~5% water, technical grade, 90%, Sigma Aldrich, St. Louis, United States), the amino acids 2-amino-2-methylpropionic acid (AMPA; 99%, Sigma Aldrich, St. Louis, United States) and sarcosine (SAR; 98%, Sigma Aldrich, St. Louis, United States), the glycol triethylene glycol (TEG; ReagentPlus, 99%, Sigma Aldrich, St. Louis, United States) and potassium hydroxide (KOH; analytical reagent grade, Fisher Scientific International Inc., Pittsburgh, United States).

The reaction of CO_2 and K_2CO_3 to $KHCO_3$ in the presence of water is described by the Equation (2). Amino species bind CO_2 by forming carbamate by Equation (3). For an efficient promoter effect, the carbamate should be as unstable as possible and be hydrolyzed quickly as shown in Equation (4) for basic solutions. This makes the amino species available for binding again and passes on the CO_2 in the form of HCO_3^- for the formation of $KHCO_3$.

$$CO_2 + K_2CO_3 + H_2O \leftrightarrow 2\ KHCO_3 \tag{2}$$
$$RNH_2 + CO_2 \leftrightarrow RN^+H_2COO^- \tag{3}$$
$$RN^+H_2COO^- + OH^- \leftrightarrow RNH_2 + HCO_3^- \tag{4}$$

Glycols and KOH have a positive effect on absorption in another way. CO_2 reacts reversibly with the hydroxide groups of the glycols, whereby CO_2 is chemically bound. In particular, the glycols also reduce the vapor pressure of the absorption medium, which counteracts its loss in the process. KOH has a positive effect on the process by renewing K_2CO_3 from $KHCO_3$ according to Equation (5).

$$KHCO_3 + KOH \leftrightarrow K_2CO_3 + H_2O \tag{5}$$

2.2 Cooling Crystallization of Dissolved $KHCO_3$

The cooling crystallization was investigated in a mixed-suspension, mixed-product-removal crystallizer. K_2CO_3/$KHCO_3$ solutions were placed in a temperature-controlled storage vessel and transferred to the temperature-controlled crystallizer vessel with overflow. Two different solutions with realistic proportions of K_2CO_3 and $KHCO_3$ after CO_2 absorption were prepared by dissolving K_2CO_3 and $KHCO_3$ (≥99, Ph. Eur., Carl Roth Gmbh + Co. KG, Karlsruhe, Germany) in demineralized water. The first solution contained 22.4 wt% K_2CO_3 and 21.6 wt% $KHCO_3$. The second solution contained 24.2 wt.% K_2CO_3 and 15.8 wt.% $KHCO_3$. The first solution was tempered to 343 K in the storage vessel, the second to 319 K. The crystallization temperatures tested were 308 K and 323 K for the first solution and 398 K and 308 K for the second. The crystallization vessel was mixed with a magnetic stirrer at 566 rpm during the experiments. The three mean residence times of 15 min, 30 min and 45 min in the crystallization vessel were investigated, which corresponded to flow rates of 100 ml/min, 50 ml/min and 33.4 ml/min. At three different times, 50 ml samples were taken from the crystallization vessel using a volumetric pipette and filtered. The first and second sample were taken after the reactor volume was exchanged two and seven times. The third sample was taken 2 h after the experiment stopped. A

https://doi.org/10.52202/077185-0132

filter funnel with a filter paper with a pore size <= 16 µm was used for filtration using a vacuum flask. The filtrates were dried overnight at 333 K in a drying oven. The dried crystallization products were separated into the size fractions < 64 µm, 64 µm - 125 µm, 126 µm - 250 µm, 251 µm - 630 µm and > 630 µm using a sieve shaking tower for 20 min at maximum intensity (analysette 03.502, FRITSCH GmbH, Idar-Oberstein, Germany) and weighted subsequently.

2.3 Thermal Decomposition of Solid $KHCO_3$

The thermal decomposition of $KHCO_3$ was carried out using a heated integral tube reactor with an inner diameter of 15 mm, a wall thickness of 1.5 mm and a length of 70 mm. The temperatures on the outer wall and in the center of the reactor were monitored with thermocouples. Different heating rates in the range of 0.0028 K/s and 0.1 K/s were tested. Two gas pipes with an internal diameter of 5 mm were flanged to the reactor. Glass wool was used to prevent the transport of solids into the gas lines. 25 g of $KHCO_3$ were used for each experiment. The gas flows through the reactor were controlled with mass flow controllers. After the reactor, the gas was dried at 278 K using a Dimroth cooler. The analog CO_2 measuring device (Binos 1, Leybold Heraeus GmbH, now Leybold GmbH, Cologne, Germany) was read out digitally using an analog-to-digital converter (Personal Daq/56, IOtech Inc., Cleveland, United States). Before each experiment, the measuring device was zeroed at room temperature and a N_2 flow of 10 l/h and then calibrated with a test gas (14 vol.% CO_2, 86 vol.% N_2, 10 l/h). During the tests, the reactor was continuously flowed with 10 l/h N_2. The influence of three different particle size fractions (63 µm - 125 µm, 126 µm - 250 µm and 251 µm - 400 µm) on the decomposition was investigated. The different size fractions were achieved using the aforementioned sieve tower. The thermal decomposition is analogous to Equation (2), but in the other direction. Decomposition kinetics were evaluated using the Arrhenius Equation (6) that consists of the rate constant k, the pre-exponential factor A, the activation energy Ea, the universal gas constant R and the temperature T.

$$k = A \cdot e^{-\frac{E_a}{R \cdot T}} \tag{6}$$

2.4 Hydrogenation of CO_2 to CH_4

The hydrogenation of CO_2 to CH_4 was carried out in the aforementioned integral tube reactor. The so-called Sabatier reaction proceeds according to Equation (7).

$$CO_2 + 4\,H_2 \rightarrow CH_4 + 2\,H_2O \tag{7}$$

The reaction A commercial catalyst with 5 wt.-% ruthenium on aluminum oxide (5 wt.-% Ru/Al_2O_3; Sigma Aldrich, St. Louis, United States) was placed as fixed bed in the center of the reactor. The reactor was then purged with 50 l/h argon (Ar) before each experiment. The catalyst was then reduced for activation. For this purpose, the reactor was first heated to 773 K in the furnace for 60 min and kept at this target temperature for 20 min. The flow of Ar was then successively replaced by hydrogen (H_2) in nine steps with 15 min intervals. The furnace was then switched off and opened for cooling. After cooling, single hydrogenation experiments were performed. During each experiment, the exhaust gas from the reactor was first cooled and then analyzed for the proportions of CO_2, CO and CH_4. The CO_2 measurement was carried out as described under 2.3. The CO content was also analyzed with the same measuring device, but without calibration using test gas. Here, the measuring range of the device was mapped in a simplified linear fashion to the range of the current variation observed during the temperature-dependent hydrogenation. The amount of CH_4 formed was determined using a pre-calibrated measuring device (Rosemount Analytical NGA 2000, Emerson Electric Co., St. Louis, United States).

For the kinetic studies of the hydrogenation, 1 g, 3 g, 5 g or 9 g of fresh catalyst were held in position by two compression springs with stainless steel perforated plates between the springs and the catalyst. The reactor was flushed with H_2 and CO_2 in a volume ratio of 2.5-to-1 at different flow rates to vary the average residence time of the gases in the catalyst bed. Different heating rates were applied to reach the target temperatures of 503 K to 743 K in 60 min to 120 min.

https://doi.org/10.52202/077185-0132

In addition, experiments were also carried out on the integrated $KHCO_3$ decomposition in the CO_2 hydrogenation. For this purpose, either 1 g or 2 g of $KHCO_3$ were placed in the front part of the reactor instead of the pressure spring in front of the perforated plate. This was followed by the catalyst, another perforated plate and pressure spring, as in the non-integrated experiments. 5 g of catalyst were used in each integrated experiment. The catalyst was reduced in H_2 before the $KHCO_3$ was added to the reactor. The three heating rates 0.058 K/s, 0.111 K/s and 0.228 K/s were tested. The reactor was flushed with 12.2 l/h H_2 during the experiments.

3 RESULTS AND DISCUSSION

In the following, the experimental results are presented and discussed according to the individual process steps. Figure 1 shows the four main steps, which are CO_2 absorption in aqueous K_2CO_3 solutions by $KHCO_3$ formation (a), cooling crystallization of dissolved $KHCO_3$ (b), thermal decomposition of solid $KHCO_3$ crystals to K_2CO_3, H_2O and CO_2 (c), and the hydrogenation of CO_2 to CH_4 (d). In a power-to-gas concept, H_2 for hydrogenation is provided from H_2O electrolysis with surplus electricity (e). The process is not examined in this work.

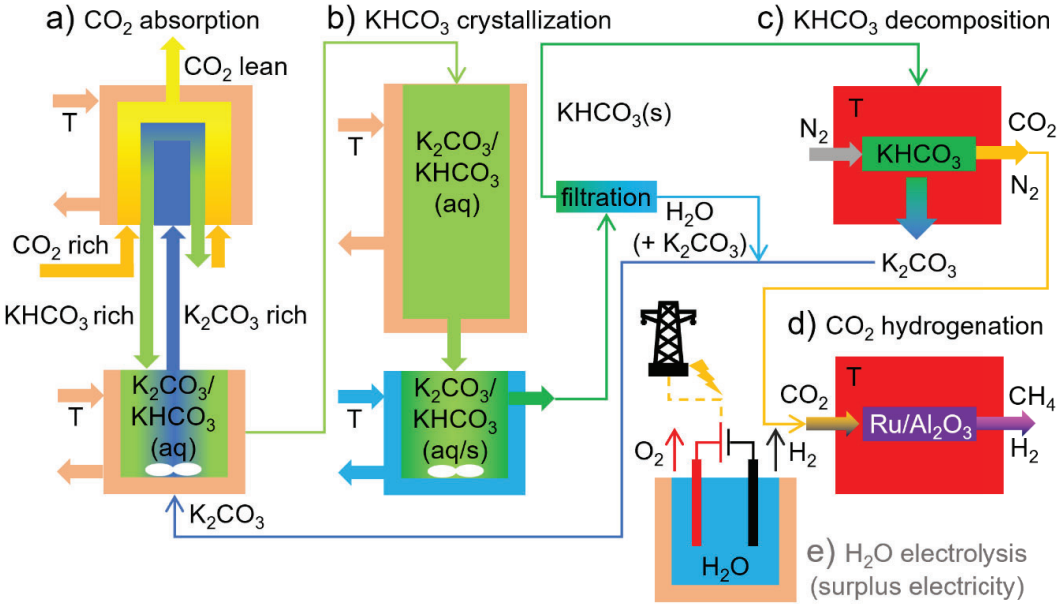

Figure 1: Sketch of the four steps of the overall process under investigation: CO_2 absorption (a), $KHCO_3$ crystallization (b), $KHCO_3$ decomposition (c) and CO_2 hydrogenation (d), completed by H_2O electrolysis with surplus electricity (e), that is not studied in this work.

3.1 Chemical Absorption of CO_2 in Aqueous K_2CO_3 Solutions

The chemical absorption of CO_2 into the K_2CO_3-$KHCO_3$ buffer system has been well studied. Compared to the amine wash, it has a much slower CO_2 uptake. However, the absorption performance can be increased to a comparable level using promoters. The influence of different types of promoters on CO_2 absorption performance was investigated for the amine piperazine (PZ), the alkanolamine 2-amino-2-methylpropanol (AMP), the amino acids 2-amino-2-methylpropionic acid (AMPA) and sarcosine (SAR) as well as triethylene glycol (TEG) and potassium hydroxide (KOH).

Figure 2a in the inlet shows the typical decrease in the mass transfer rate over time. The synergistic effect of K_2CO_3 and the amino species, here exemplified by AMPA, on CO_2 absorption is also clearly shown. The alkanolamine had a significantly higher absorption performance than K_2CO_3 at the beginning. However, K_2CO_3 absorbed significantly longer than the amine. In combination, the two properties complemented each other and exceeded a pure summation of the mass transfer rates. For the further comparison of promoters, the mass transfer rates of the first few minutes were used, even if the

https://doi.org/10.52202/077185-0132

time course of the mass transfer rate decreased to varying degrees. The reason for this is that the continuous exchange of loaded absorption fluid with unloaded absorption fluid in the application will always secure high mass transfer rates. In further comparison, various effects were observed. Firstly, an increase in CO_2 uptake could not be achieved with higher concentrations than 1 M K_2CO_3. This was also true in combination with AMP and AMPA. Only with PZ was a positive effect observed. An increase was also achieved with TEG. A synergistic effect with K_2CO_3 was not evident. In general, the best results were achieved with SAR in combination with KOH as well as with PZ. In general, the combination of K_2CO_3 and amino species often only had a positive effect after longer test durations.

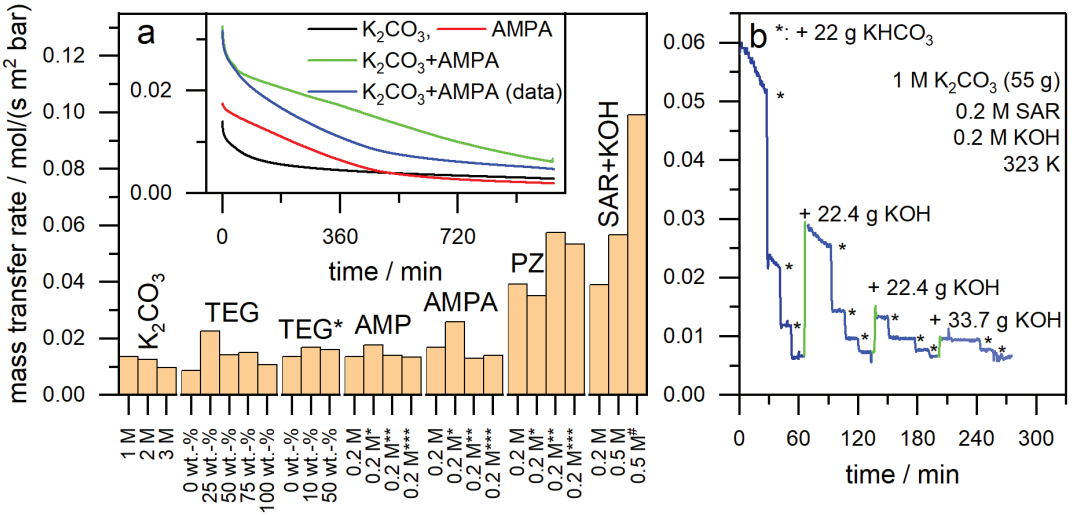

Figure 2: Initial mass transfer rates for different absorption media with inlet showing mass transfer rates over time for 1 M K_2CO_3, 0.5 M AMPA, their mixture and the summed-up data as control (a) and mass transfer rate over time for mixture of K_2CO_3, KOH and SAR with repetitive additions of $KHCO_3$ and KOH (b). In (a), for each asterisk (*) 1 M K_2CO_3 was in the solution and # marks a solution containing 1 M K_2CO_3 and 10 wt.-% TEG.

In further experiments, $KHCO_3$ was added in steps to the absorption medium followed by KOH for several times (Figure 1b). The absorption medium initially contained KOH and SAR at 0.2 M each. The experiment was carried out at 323 K. The purpose of the experiment was to demonstrate the effect of different ratios of K_2CO_3 and $KHCO_2$ on CO_2 absorption and the positive effect of K_2CO_3 regeneration by KOH. The data clearly show how the addition of $KHCO_3$ leads to an abrupt reduction in CO_2 uptake. The addition of KOH then abruptly increased the mass transfer rate again. The effects can be explained by the equilibria between carbonate and hydrogen carbonate and between carbamate and hydrogen carbonate. For high CO_2 uptake, the proportion of hydrogen carbonate must be kept low, which was achieved by adding KOH.

In summary, the mass transfer rate of CO_2 can be increased to varying extent by the different promoters tested. Amino species and KOH proved to be particularly suitable. The highest mass transfer rate of about 0.1 mol/(s m² bar) was achieved with an absorption medium consisting of 1 M K_2CO_3, 0.5 M KOH, 0.5 M SAR and 10 wt.-% TEG under atmospheric conditions. In addition, the equilibrium character of the K_2CO_3/$KHCO_3$ system and the positive effect of KOH were demonstrated. In the future, CO_2 absorption should be investigated with continuous renewal of the absorption medium. In addition, the cycling of the absorber media should be tested, both after CO_2 desorption from the liquid phase and especially after desorption from the crystallized $KHCO_3$, which is discussed in more detail in 3.2. If, contrary to expectations, stable carbamates do form, these would gradually reduce the performance of absorption. In addition, application-oriented reactor concepts must be tested in the next step.

https://doi.org/10.52202/077185-0132

3.2 Cooling Crystallization of Dissolved $KHCO_3$

The use of the K_2CO_3-$KHCO_3$ buffer system in CO_2 absorption enables the intermediate storage of CO_2 in a harmless solid that can be stored and transported by crystallizing $KHCO_3$. However, this requires additional investment in crystallization. In addition, the nature of the crystallization product could have an effect on the subsequent decomposition, which is considered in 3.3. Therefore, the grain size distribution of the dried crystallization products and the cooling effort required for crystallization were primarily studied.

The grain size distribution of crystallization products of aqueous solutions with two different KCO_3-to-$KHCO_3$ ratios were investigated. Both solutions contained about 23 wt.-% K_2CO_3. The ratio of K_2CO_3-to-$KHCO_3$ was about 1-to-1 for the first solution and 1-to-0.67 for the second. The solutions were only completely clear at 343 K (1-to-1) or 318 K (1-to-0.67), respectively. These temperatures served as feed temperatures to avoid crystallization in the feed. Other varied parameters were the temperature difference between crystallization reactor and feed and the residence time in the reactor. First of all, Figure 3a shows typical grain size mass distributions after sampling at three different times of the experiment. Shown is the median of a threefold measurement with absolute deviation in the form of error bars. It can be clearly seen that about half of the mass is present in the fraction 126 µm - 250 µm. The rest of the mass is distributed approximately equally between the larger and smaller fractions. Also obvious is the wide scatter, which would overlay an existing trend on the duration of the test. It could be due to fluctuations in sampling from the reaction volume, which is difficult with the type of process and reactor. The distribution originates from the drying product of the 1-to-1 solution at 30 min mean residence time and 20 K temperature difference. However, it hardly deviates from those of the other parameter sets within the fluctuation range. Only the composition of the solution shows a small effect in that the size distribution shifts slightly towards smaller particle sizes (Figure 3b). The 64 µm – 125 µm fraction increases in mass at the expense of the 126 µm - 250 µm fraction.

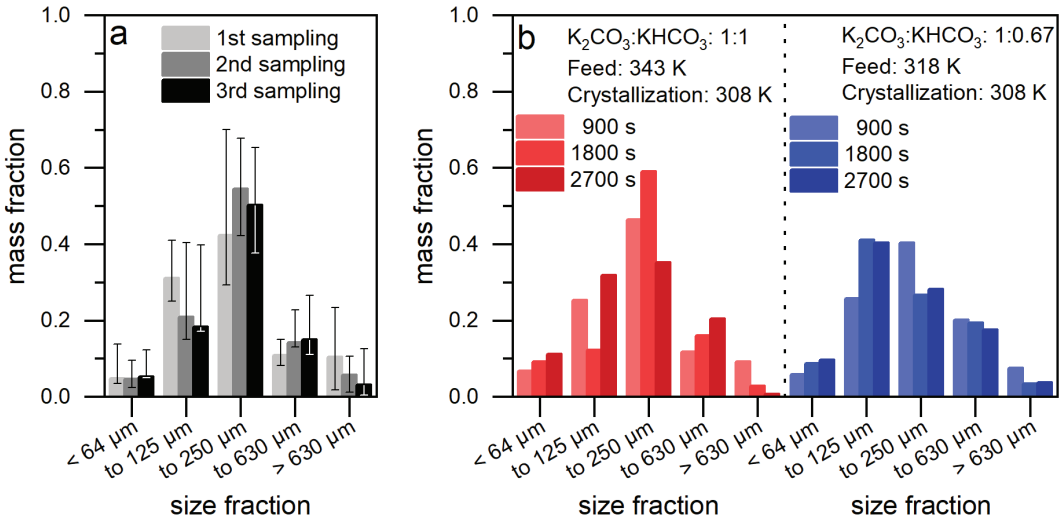

Figure 3: Grain size distribution for K_2CO_3:$KHCO_3$ 1:1, 323 K crystallization temperature showing the medians of a threefold measurement with maximum deviation as error bars for three samples taken at different times of experiment (a) and two exemplary grain size distributions for the two different K_2CO_3:$KHCO_3$ ratios and three different mean residence times (b).

Neither the K_2CO_3-to-$KHCO_3$ ratio, the feed temperature nor the temperature difference between the feed and the crystallization reactor had any clear influence on the yield, which averaged 1.16 for 35 measurements, with a minimum of 0.82 and a maximum of 1.74. The time of sampling and the average residence time also had no apparent influence. The wide scatter again refers to the difficulty of sampling. However, based on the mean value, it can largely be assumed that the reactor was close to

https://doi.org/10.52202/077185-0132

equilibrium under the test conditions. With reference to the cooling energy to be used, it can be said that this can probably be further minimized if the throughput is not increased.

In summary, it can be said that either the lower $KHCO_3$ content or the associated lower feed temperature has a positive effect on the process by resulting in the formation of smaller crystals. The effect should be investigated further. The lower feed temperature is advantageous in terms of energy. However, the small amount of $KHCO_3$ means that an unnecessarily large amount of KCO_3 has to be circulated in the process. In future, the influence of the promoters on crystallization should be investigated. In addition, the question of a possible coupling of crystallization and CO_2 absorption arises. The additional energy or time required for cooling could be avoided since crystallization through supersaturation must take place in the process anyway. However, new challenges would then have to be overcome in terms of process flow control.

3.3 Thermal Decomposition of Solid $KHCO_3$

$KHCO_3$ can be thermally decomposed to solid K_2CO_3, H_2O and gaseous CO_2. After drying the CO_2, it is therefore available in high purity as a starting material for hydrogenation reactions, for example. In addition, K_2CO_3 is obtained, which can be used again in aqueous solution to absorb CO_2 from emission sources. Decomposition is an energy-intensive step in the overall process. Against this background, the influence of the grain size distribution on the decomposition energy required was of particular interest. The speed of the reaction is also of interest when for an outlook on upscaling.

The reaction kinetics of the decomposition of $KHCO_3$ were studied for three size fractions in the range from 63 µm to 400 µm at a constant, low heating rate of 0.0029 K/s (Figure 4a). In all cases, the kinetics followed a first-order reaction in the temperature range 392 K - 425 K. The activation energies were in the range of 91.9 kJ/mol - 96.1 kJ/mol. The pre-exponential factors were in the range of 16.7 ln(1/s) and 17.9 ln(1/s). Activation energies and pre-exponential factors were independent from the grainsize. The values are in good agreement with results from the literature, which are 92.8 kJ/mol and 18.9 ln(1/s) (Tanaka, 1987).

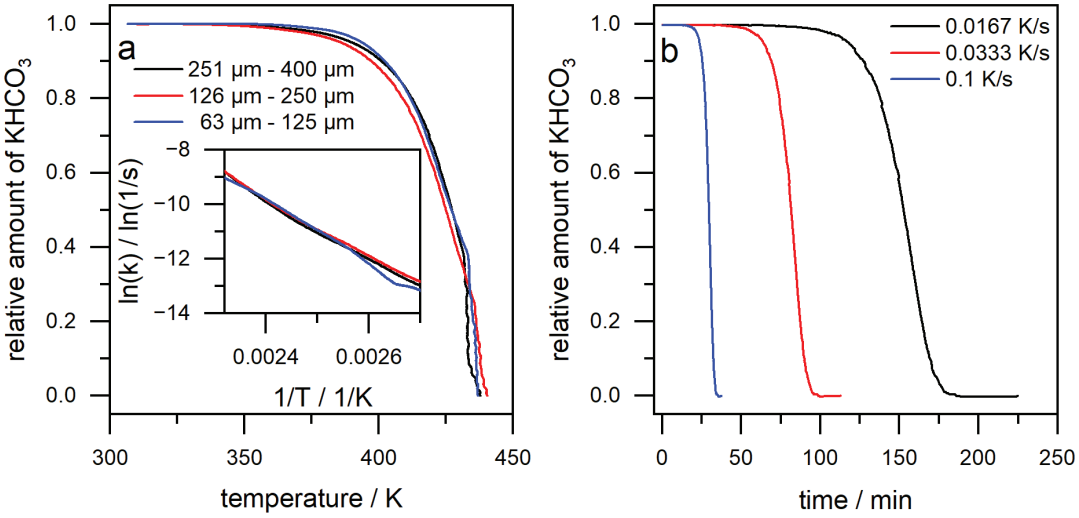

Figure 4: Amount of $KHCO_3$ left during thermal decomposition versus temperature for three grain size fractions with inlet showing the Arrhenius plot (a) and amount of $KHCO_3$ left during thermal decomposition at three heating rates (b).

Further, the influence of different heating rates on the decomposition of $KHCO_3$ was investigated without size fractioning. It was found that the decomposition was accelerated with increasing heating rate but a slightly lower pace (Figure 4b). Full decomposition was achieved with a relative delay of 0.06

https://doi.org/10.52202/077185-0132

when the heating rate was doubled from 0.0167 K/s to 0.0333 K/s and with a relative delay of 0.14 when the heating rate was increased sixfold. This also results in higher final temperatures in the reactor of 488 K and 502 K, compared to 478 K. Slow heat diffusion through individual grains and, in particular, the total bed can be cited as the reason.

In summary, there was no effect of the grain size on the decomposition rate in the investigated range of 63 µm to 400 µm. The increase in the heating rate contributed to the acceleration of decomposition, but with some sluggishness. In future studies, the heat diffusion should be optimized not only by small grain sizes, but also in particular by low layer thicknesses of the bed. Decomposition at constant temperatures should also be investigated.

3.4 Hydrogenation of CO_2 to CH_4

The hydrogenation of CO_2 to CH_4 is of interest because CH_4 makes up the majority of natural gas and the hydrogenation product can therefore be fed into the existing grid if it is highly pure. Hydrogenation can be operated with electrolysis hydrogen when there is a surplus of electricity and is therefore considered an electricity storage system in the sense of the power-to-gas concept. In addition, thermal energy is required for both the hydrogenation and the preceding decomposition. An integrated operation of both processes would be interesting. Conversion and selectivity of the catalytic hydrogenation and the possibility of integrating $KHCO_3$ decomposition into hydrogenation were examined.

First, the temperature-dependent conversion of externally supplied CO_2 and H_2 in a volume ratio of 1 to 2.5 were studied by variation of the residence time of the gases in the catalyst bed and the amount of catalyst. The conversion of CO_2 (and H_2) to CH_4 via Ru/Al_2O_3 generally behaved logistically, as shown in the inlet Figure 5a as an example for a mean residence time of 183 ms. Here, a complete conversion to CH_4 was achieved at about 623 K. Complete conversion was observed for all residence times investigated. The temperature at which maximum conversion was achieved, decreased exponentially with increasing mean residence time, approaching 511 K asymptotically (Figure 5a).

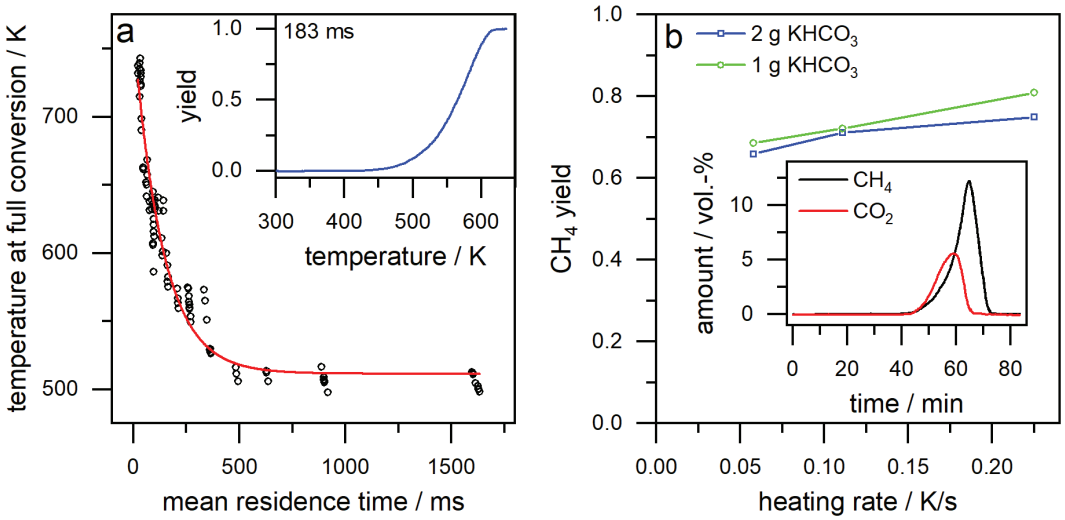

Figure 5: Temperature at full conversion of CO_2 to CH_4 versus mean residence time with inlet showing exemplary conversion curve at a residence time of 183 ms (a) and CH_4 yield versus heating rate for two amounts of $KHCO_3$ with inlet showing exemplary evolution of CH_4 and CO_2 amount over time for a heating rate of 0.058 K/s and 2 g $KHCO_3$ (b).

The amount of catalyst used had only minor influence on the conversion and the required temperature. Figure 5a shows very clearly descending point data sequences at high residence times. These are decreasing and not straightly falling, as the catalyst layer also increases in thickness with increasing

https://doi.org/10.52202/077185-0132

mass and therefore the residence time increases. The temperature at complete decomposition drops by 20 K - 50 K when the catalyst quantity is increased by a factor of 9, depending on the residence time. From this it can be concluded that the amount of catalyst or at least the loading of Ru on Al_2O_3 can still be significantly reduced, which would lower the operating costs.

The formation of CO was below 0.05 vol.-% in all experiments. Only in the case of very short residence times and thus high temperatures for full conversion, formation of 0.25 vol.-% CO was observed. Ru is known for a high selectivity in CO_2 methanization (Solymosi *et al.*, 1981; Mutschler *et al.*, 2018).

In the case of the integration of the $KHCO_3$ decomposition into the hydrogenation, the formation of CH_4 for three different heating rates was demonstrated (Figure 5b). An example of the formation of CH_4 and also CO_2 at a heating rate of 0.058 K/s is shown in the inlet of Figure 5b. It can be seen very clearly that not all CO_2 is converted to CH_4. As the heating rate was increased, the yield of CH_4 increased from about 0.67 to about 0.8, as decomposition and hydrogenation overlapped more in time. A lower amount of $KHCO_3$ with the same amount of catalyst proved to be advantageous.

In summary, full conversion with very high selectivity was achieved using a commercial Ru/Al_2O catalyst. A compromise must be made between CH_4 productivity (via the residence time) and heating energy consumption. In future studies, the amount of catalyst used should be minimized. In addition, stability tests should be investigated, taking into account long running times and repeated starting of the process. In addition, the coupling of residence time and productivity is unfavorable and could be addressed using different reactor dimensions. Furthermore, the coupling of hydrogenation and $KHCO_3$ decomposition was successfully demonstrated. The process was favored by fast heating rates and a lower proportion of $KHCO_3$ compared to the catalyst. In the future, the influence of residues of amino acid promoters in $KHCO_3$ should be investigated. These could result in the formation of nitrogen oxides. In addition, the coupling of the processes requires a regular exchange of the reacted $KHCO_3$.

4 CONCLUSIONS

The scrubbing of CO_2-rich exhaust gases, for example from power plants, from other plants that burn conventional energy sources or from biogas plants, can make an important contribution to the required rapid reduction of greenhouse gas emissions. Here, a novel absorption-desorption process with a more economical and ecological K_2CO_3-based absorber medium compared to conventional amine-based ones was demonstrated. The process also creates more flexibility in the application with solid $KHCO_3$ as an intermediate CO_2 storage medium. In particular, the energy required for desorption can be separated from absorption in terms of time and location if required. This means that desorption for CO_2 supply can be carried out specifically when there is excess electricity for hydrogen production by means of electrolysis. Hydrogenation of CO_2 then makes hydrocarbons accessible, such as CH_4, which can be fed into the natural gas grid. The other main product of the decomposition, the initial carbonate, can be used to refresh the absorber solution. In addition to the decoupled hydrogenation of CO_2 over Ru/A_2O_3, in which 100% yield and selectivity were achieved, hydrogenation and $KHCO_3$ decomposition were successfully coupled too. Conversion of 80% was achieved in the coupled approach. Optimization of the process control should enable 100% conversion in future too.

NOMENCLATURE

A	pre-exponential factor	(-)
Ea	activation energy	(J/mol)
J	molar flow density	(mol/(s m²))
k	rate constant	(1/s)
p	partial pressure	(bar)
r	mass flow rate	(mol/(s m² bar)
R	universal gas constant	(8.3145 J/(mol K))
T	temperature	(K)

https://doi.org/10.52202/077185-0132

REFERENCES

Aghel, B., Janati, S., Wongwises, S., Shadloo, M.S., 2022, Review on CO2 capture by blended amine solutions, *International Journal of Greenhouse Gas Control*, vol. 119: p. 103715.

Ahmed, R.E., Wiheeb, A.D., 2020, Enhancement of carbon dioxide absorption into aqueous potassium carbonate by adding amino acid salts, *Materials Today: Proceedings*, vol. 20: p. 611-616.

Astarita, G., Marrucci, G., Gioia, F., 1964, The influence of carbonation ratio and total amine concentration on carbon dioxide absorption in aqueous monoethanolamine solutions, *Chemical Engineering Science*, vol. 19, no. 2: p. 95-103.

Culliane, J.T., Oyenekan, B.A., Lu, J., Rochelle, G.T., 2005, Aqueous piperazine/potassium carbonate for enhanced CO2 capture, *Greenhouse Gas Control Technologies 7*, vol. I: p. 63-71.

Gouedard, C., Picq, D., Launay, F., Carrette, P.-L., 2012, Amine degradation in CO2 capture. I. A review, *International Journal of Greenhouse Gas Control*, vol. 10: p. 244-270.

Hikita, H., Asai, S., Katsu, Y., Ikuno, S., 1979, Absorption of carbon dioxide into aqueous monoethanolamine solutions, *AIChE Journal*, vol. 25, no. 5: p. 793-800.

Hirst, L.L., Pinkel, I.I., 1936, Absorption of Carbon Dioxide by Amines Di- and Triethanolamine and Tetramine, *Ind. Eng. Chem.*, vol. 28, no. 11: p. 1313-1315.

Hook, R.J., 1997, An Investigation of Some Sterically Hindered Amines as Potential Carbon Dioxide Scrubbing Compounds, *Ind. Eng. Chem. Res.*, vol. 36, no. 5: p. 1779-1790.

Killeffer, D.H., 1937, Absorption of Carbon Dioxide, *Ind. Eng. Chem.*, vol. 29, no. 11: p. 1293.

Liu, Z., Deng, Z., Davis, S., Ciais, P., 2023, Monitoring global carbon emissions in 2022, *Nat Rev Earth Environ*, vol. 4, no. 4: p. 205-206.

Liu, Z., Deng, Z., Davis, S.J., Giron, C., Ciais, P., 2022, Monitoring global carbon emissions in 2021, *Nat Rev Earth Environ*, vol. 3, no. 4: p. 217-219.

McCoy, H.N., Smith, H.J., 1911, EQUILIBRIUM BETWEEN ALKALI-EARTH CARBONATES, CARBON DIOXIDE AND WATER, *J. Am. Chem. Soc.*, vol. 33, no. 4: p. 468-473.

Mutschler, R., Moioli, E., Luo, W., Gallandat, N., Züttel, A., 2018, CO2 hydrogenation reaction over pristine Fe, Co, Ni, Cu and Al2O3 supported Ru: Comparison and determination of the activation energies, *Journal of Catalysis*, vol. 366: p. 139-149.

Ochedi, F.O., Yu, J., Yu, H., Liu, Y., Hussain, A., 2021, Carbon dioxide capture using liquid absorption methods: a review, *Environ Chem Lett*, vol. 19, no. 1: p. 77-109.

Sang Sefidi, V., Luis, P., 2019, Advanced Amino Acid-Based Technologies for CO 2 Capture: A Review, *Ind. Eng. Chem. Res.*, vol. 58, no. 44: p. 20181-20194.

Sartori, G., Savage, D.W., 1983, Sterically hindered amines for carbon dioxide removal from gases, *Ind. Eng. Chem. Fund.*, vol. 22, no. 2: p. 239-249.

Solymosi, F., Erdöhelyi, A., Kocsis, M., 1981, Methanation of CO2 on supported Ru catalysts, *J. Chem. Soc., Faraday Trans. 1*, vol. 77, no. 5: p. 1003.

Tanaka, H., 1987, Comparison of thermal properties and kinetics of decompositions of $NaHCO_3$ and $KHCO_3$, *Journal of Thermal Analysis*, vol. 32: p. 521-526.

Tseng, P.C., Ho, W.S., Savage, D.W., 1988, Carbon dioxide absorption into promoted carbonate solutions, *AIChE Journal*, vol. 34, no. 6: p. 922-931.

Williamson, R.V., Mathews, J.H., 1924, Rate of Absorption and Equilibrium of Carbon Dioxide in Alkaline Solutions, *Ind. Eng. Chem.*, vol. 16, no. 11: p. 1157-1161.

ACKNOWLEDGEMENT

We thank the Federal Ministry for Economic Affairs and Climate Protection of the Federal Republic of Germany for supporting our research with funding in the BiCarb2Fuel project (funding reference code: 03EE5053A). In addition, we thank the students Mustafa Elemen, Hatun Erciyes, Ante Giljanovic, Sebastian Jonczyk, Dhay-Parn Lou, Hüseyin Mintas, which conducted experiments, simulations, and literature research in the frame of the project.

https://doi.org/10.52202/077185-0132